

UNPUBLISHED PRELIMINARY DATA

UNIVERSITY OF



GPO PRICE \$ _____

OTS PRICE(S) \$ _____

Hard copy (HC) 2.00

Microfiche (MF) .50

LAND

FACILITY FORM 602

N65-26024

(ACCESSION NUMBER)

48

(PAGES)

CR 63379

(NASA CR OR TMX OR AD NUMBER)

(THRU)

1

(CODE)

11

(CATEGORY)

THE INSTITUTE FOR FLUID DYNAMICS

and

APPLIED MATHEMATICS

Technical Note BN-353

April 1964

DEVELOPMENT OF A SPECTROSCOPIC
SHOCK TUBE*

by

M. H. Miller and T. D. Wilkerson

University of Maryland
College Park, Maryland

*This research was supported in part by the National Aeronautics and Space Administration under Grant NSG 359 and by the United States Air Force under Grant AFOSR 141-63.

TABLE OF CONTENTS

	<u>Page</u>
I. Introduction	1
II. Scientific Background and Objectives	1
III. Construction of Shock Tube	3
A. Factors Determining Shock Tube Design	3
B. Description of Shock Tube	5
IV. Gas Delivery and Evacuation Equipment	9
A. High Pressure System	9
B. The Vacuum System	10
V. Shock Tube Instrumentation	12
A. Location of Observation Stations	12
B. Film Strip Resistors	13
C. Pressure Transducers	14
D. Wave Speed Photography	15
E. Spectrographs	16
F. Calibrated High Intensity Flash Lamp	18
VI. Shock Tube Data Collected	19
A. Performance of The Vacuum System	19
B. Diaphragm Testing	20
C. Hydrodynamic and Spectroscopic Performance of Shock Tube	21

TABLE OF CONTENTS - continued

	<u>Page</u>
VII. Research Activities for the Current Year	25
A. Development Work in Progress	25
B. Experiments in Progress	26
C. Spectroscopic Studies of the Current Year	27
D. Projected Plans for Research in 1965	28
List of Figures	30
Annotated Bibliography	31

ABSTRACT

26024

We describe a gas-driven shock tube and associated equipment to be used for radiative transfer experiments in the Institute for Fluid Dynamics and Applied Mathematics, University of Maryland. This report covers the design and construction of the tube and its initial operation to check out the hydrodynamic behavior. Various devices measure the flow properties. We achieve temperatures up to $15,000^{\circ}\text{K}$, for periods up to 300 microseconds, in the stationary gas behind the reflected shock wave. These conditions allow meaningful reduction of emission spectra to absolute line strengths for many elements of astrophysical interest. Other radiative transfer problems will also be studied. We discuss preliminary spectroscopic work and the instruments now being built for time-resolved spectroscopy.

Author

I. INTRODUCTION

We have built a new spectroscopic shock tube and operated it successfully over the ranges of temperature and density required for spectral measurements. Our aims are to determine atomic oscillator strengths, to compare emission and absorption coefficients, and to correlate the hydrodynamics and emissivity of the shock-heated gases. Some aspects of these problems are discussed in Section II. Sections III and IV, respectively, are devoted to the construction and design of the shock tube and its auxiliary system for filling and evacuation. Section V deals with the instruments for observing the high speed gas flows; some of these are now operating and others are under development. Preliminary data on shock tube operation are given in Section VI. Section VII covers both the immediate problems and the work projected for the near future. At this time, the prospects appear quite good for collecting data of use in astrophysics. This research is conducted both by faculty members and graduate students working toward advanced degrees.

II. SCIENTIFIC BACKGROUND AND OBJECTIVES

The most difficult problem in radiation experiments has been to create spectroscopic sources of known composition, temperature T , emitter and electron densities, n and n_e , which are sufficiently homogeneous and stable during the measurement period that the state variables are both well defined and measurable.

Our first objective is to produce such a well calibrated spectroscopic source. Shock tubes are convenient for producing gas samples at temperatures high enough for atoms and ions to be excited. In a conventional shock tube, the gas sample formed behind the reflected shock wave is homogeneous over a large volume and persists in a steady state for a sufficient period to allow direct measurement of the state variables. We plan to measure each variable by several methods. Temperature will follow from relative and absolute line intensities, and by the reversal method employing a calibrated, high intensity, flash lamp. Densities will be determined by spectroscopy and optical interferometry. Composition is controlled by the partial pressures of gases admitted into the tube.

In principle, the Rankine-Hugoniot equations predict gas temperature and density behind the reflected shock from the compositions and pressures of the driving gas and test gas. These one dimensional, ideal gas equations, however, neglect real-gas effects and boundary layer interactions. Useful temperature and density predictions may still be extracted if the equations are fitted to the (locally) observed incident and reflected shock speeds (U and V), the initial flow velocity u_1 and the pressures, p_1 and p_2 behind the incident and reflected shock, respectively.

With the source variables T , n and n_0 known, (and given that criteria for local thermal equilibrium are fulfilled), absolute spectral intensity measurements will yield atomic oscillator strengths with precisions in the range 10% - 20%. Other studies bearing on atomic relaxation rates and radiative transfer likewise require a well-known gas as the spectroscopic source, and we expect to work on these at the appropriate time.

III. CONSTRUCTION OF THE SHOCK TUBE

A. Factors Determining Shock Tube Design.

1. Choice of a Rectangular Cross-Section.

A rectangular cross-section simplifies analysis of data gathered optically from the shock tube. Spectroscopic information is gathered from everywhere within a small solid angle traversing the tube perpendicularly to the tube axis. The boundary layer forms a sheath near the walls which is in a different state than the bulk of gas being viewed. Plane walls form plane boundary layers, providing a far simpler geometry for analysis of source radiation than possible with a tube of round cross-section. If light is gathered from two paths of unequal length at the same point along the tube axis, one can assess the boundary layer contributions to the emission and absorption spectra.

2. Factors Determining Shock Tube Reinforcement and Size.

The inside tube dimensions were chosen to minimize shock attenuation due to boundary layer losses. For a given combination of driver and test gases, the Mach number achieved in ideal, one-dimensional flow depends only upon the ratio of driver gas initial pressure p_0 to test gas initial pressure p_1 . Shocks propagated in tubes of finite cross-section, however, suffer attenuation due to boundary layer growth. This attenuation increases with larger surface-to-volume ratio, so it is best to have the largest cross-section possible within the limits set by structural strength and the operating cost-per-shot. The present tube has the inside dimensions of 3.64" in the vertical direction and 2.64" in the horizontal direction.

3. Desirability of High Working Pressure.

The present tube was designed to withstand maximum delivery pressure from commercial gas cylinder, 1800 - 2200 psi. Since test gas initial pressure cannot be lowered without shortening the life of the steady state region behind the reflected wave, the limit of Mach number achieved is set by the capability of the driver section to withstand high pressure.

+. Other Design Considerations.

Design details of the shock tube, not all of which will be discussed, were dictated by the following:

- a. Need for uniform cross-section in the flow channel.
- b. Need for highest vacuum obtainable with the construction materials and pumping systems available.
- c. Flexibility of design to allow future alterations of the system.
- d. Desirability of running many experiments per day.

B. Description of the Shock Tube.

1. Overall Dimensions.

The shock tube (unreinforced) has outside dimensions of 3" x 4". Inside dimensions are 3.64" x 2.64". Inside corner radii are 0.010". The driver section has an inside length of 48". The total length of the expansion section is 150", comprised of a 10" breech section, 2 interchangeable sections of 58" each, connected in tandem, and a test section of length 24". Figure 1 views the tube diagonally from test section to driver section.

2. Material Used.

The unreinforced tube, except for the breech section, is mild steel rectangular tube, resistance welded with inside flash removed.

Wall thickness is 0.180". Mean inside surface roughness (measured with a Brush Surface Tester) is 125 micro-inches. The tube is cadmium-plated to retard oxidation. Flanges are cut from 1" mild steel plate and the breech section is machined from a 9" x 9" x 10" mild steel billet. Reinforcing materials are described below.

3. Tube Reinforcement.

a. Need for Reinforcing The Tube.

Hydrostatic testing of the 0.180" wall thickness tube, the heaviest available with a 3" x 4" cross-section, showed unacceptably large deformation at modest pressures and tube rupture near the desired maximum working pressure. Internal pressure causes the tube to swell in its effort to assume an elliptical cross-section. The percent elongation of the line joining the midpoints of the 4" sides was 0.4% at 200 psi, 1% at 400 psi, and 4.5% at 600 psi. Cold-working at the corners resulted in tube rupture at 2,800 psi. The reinforcing described below cut deformation to acceptable levels and showed no evidence of elastic hysteresis. Measured percent elongation for the reinforced expansion sections are: 0.13% at 200 psi, 0.26% at 400 psi and 0.39% at 600 psi. Installation of instrument parts has proved relatively simple with the reinforcing used.

b. Reinforcing of Driver Section.

In making the driver section, a thick-walled outer pipe gives support to the thin-walled inner tube. The 3" x 4" tube was inserted coaxially within a mild steel, circular cylinder of 5-1/2" I.D. and 1/2" wall thickness. The space between the tubes was filled with a high density, small aggregate concrete, capable of 2700 psi compression loading, prepared by the Sand and Gravel Institute, University of Maryland. Figure 2-a is a schematic cross section of the reinforced driver. This heavy driver section is mounted on roller bearings to provide easy access to the diaphragm breech.

c. Reinforcing Expansion Sections.

The expansion sections differ in reinforcement from the driver, since expansion sections need withstand only 1/4 the driver pressure, and the fitting of diagnostic ports and windows through the concrete would pose a difficult problem. The 3" x 4" tube is sandwiched between mild steel bar stock. The bar stock is forced against the tube by heavy bolts retained in square clamps encircling the tube. The arrangement is shown in Figures 2b and 3. The bar stock used on the top and bottom faces is 1/2" x 3" and that used laterally is 1" x 3". To mount diagnostic ports or windows, appropriate size holes are cut through the reinforcing bars and the face of the tube at the site of the port (window) is faced flat

with an end mill. O-rings carried in the shoulder of the port (window) seal against the prepared face. Windows and diagnostic ports are held in place by hold-down rings anchored in the reinforcing bar. Figure 3 shows a diagnostic port site.

4. Breech Section

The breech section holds the diaphragm and also serves as the junction between the shock tube and vacuum system. It is machined from a mild steel billet and has inside dimensions milled to match the adjoining expansion section. The diaphragm retaining portion, facing the driver, has three concentric ridges of height 0.005" which bite into the perimeter of the diaphragm and prevent creep under pressure. The insertion of diaphragms is facilitated by breech-locking nuts which require only slackening for removal, and by tapered pins which aid in fast driver-to-breech alignment. These are shown in Figure 4.

5. The Test Section

The present test section is similar in construction to the other two expansion sections except for its shorter length and the fitting of the lateral windows. The test section is terminated with an elongated plug which advances the reflecting plane of the shock tube into the field of view of the lateral windows. This plug is welded to the

terminating flange and protrudes 4" upstream from it, mating with the inside of the tube to within 0.003". Figure 7 is a side view of the test section, showing a window.

IV. GAS DELIVERY AND EVACUATION EQUIPMENT

A. The High Pressure System

The source of high pressure gas, usually hydrogen, is commercial tanks with delivery pressure in the range of 1800-2200 psi. Gas is fed into the tube by a high pressure flexible hose passing through the driver section's end-flange. Flow rate is regulated by a needle valve. A second flexible hose passing through the end-flange connects with an 18", 0-2000 psi, Heise bourdon gauge. Six feet of 0.020" I.D. stainless steel capillary tube constitutes the gauge's shock protection. A shut-off valve isolates the capillary and gauge from the tube during evacuation. A piston valve, also mounted on the end flange, gives a positive shut-off for the pressurized driver, while affording a reasonable conductance for driver evacuation.

A high pressure exhaust line, fitted with a quick opening toggle valve, vents the hydrogen outside of the building after each shot. Hydrogen remaining in the tube at ambient pressure is then exhausted through a mechanical vacuum pump fitted with an outdoor vent.

B. The Vacuum System

1. Pumps

A 4" PMC 720 diffusion pump, operating with Monsanto OS-124 oil, evacuates the tube in the molecular region. The diffusion pump is assisted by a BC-40 Chevron Baffle cooled to -13°C by a 1/4 HP freon-filled compressor. A 15 cubic foot/min. Duo-Seal pump alternately roughs-down the system and backs the diffusion pump. A 2-1/2" Kane molecular sieve in the fore-line prevents back-flow from the mechanical pump.

2. Vacuum Path and Valves

A 6" diameter manifold connects the vacuum system with the shock tube. The lower end of the manifold joins with the Chevron baffle after passing through a 4" CVC gate valve. The manifold has four O-ringed flanges. One of these enters a submanifold containing all vacuum gauges, except for a Pirani gauge mounted in the fore pump line. This submanifold can be isolated from the manifold by a 1" Goddard soft-seat valve. Another flange, also fitted with a 1" Goddard valve, connects with a second submanifold where gases are mixed and metered before entering the tube. The remaining flanges are the stations for dry-nitrogen backfilling and mass-spectrometer leak detecting. The manifold contains a small, externally vented breech holding a diaphragm, set to blow out should the

vacuum system accidentally be pressurized to more ~~than~~ 60 psi. The manifold's upper end connects to the shock tube breech through an Arrowflow piston closing valve with bellows-sealed stem. Figures 5 and 6 show the vacuum system and other accessory equipment.

3. Vacuum Gauges

Measurement of carrier-gas pressures, routinely in the range of 5 to 30 mm/Hg, is made with 0-20 mm/Hg and 0-100 mm/Hg Wallace and Tiernan diaphragm gauges. A four channel, LKB Pirani gauge and a CVC (10^{-4} mm/Hg- 10^{-8} mm/Hg) ionization gauge measure vacuum base pressure and the partial pressures of test gases added to the carrier gas. Periodic calibration of gauges is provided by an oil manometer and liquid nitrogen-trapped CVC McLeod gauge with useful range of 1×10^{-5} mm/Hg-10 mm/Hg.

C. Carrier Gases and Spectroscopic Additive Gases

Gases for shock tube heating will almost always consist of a rare gas (the carrier) plus a small percentage of gas of spectroscopic interest (the additive). A typical mixture might be 10 mm/Hg of Argon and 0.04 mm/Hg of Methane.

Research Grade carrier gases are drawn from tanks supplied by Matheson. Gas for immediate use enters the mixing submanifold through Nupro Fine Metering valves, and from there enters the shock tube. For

storing pre-mixed gases, we use two-liter, high pressure flasks which are chromium-plated steel with O-ringed flanges that can be removed for internal cleaning. Preliminary evacuation of flasks is through 1" stainless steel tube connecting with main manifold and sealed with a 1" Goddard soft-seat valve.

Spectroscopic additives that are gases at STP may be obtained commercially and are handled the same way as the carrier gases. Spectroscopic additives occurring as liquids or solids at STP are introduced into the shock tube by utilizing their vapor pressures. Known abundance in the gas phase is provided by vapor pressure data or pressure measurement. Time is allotted to establish phase equilibrium of the sample in a flask maintained a few degrees below room temperature by a thermostatic bath. On being admitted to the shock tube, the vapor will assume the tube's higher temperature and will not condense on the walls.

V. SHOCK WAVE INSTRUMENTATION

A. Location of Observation Stations

Figure 6 shows the location of existing and proposed diagnostic ports and windows. Film strip resistor plugs, pressure transducer plugs and photo-cell windows will fit any of the diagnostic ports of the dorsal surface of the shock tube. In its present version, the test section has

provision for optical interferometry along a single vertical path 2-1/2 cm. upstream from the tube's reflecting plane. Drum cameras, spectrographs and the calibrated continuum flash lamp are all mobile and may be situated to take best advantage of windows (two viewing laterally, and one axially).

B. Film Strip Resistors

1. Description and Construction

Film strip resistors register thermal signals by resistive changes induced in a metal film of low specific heat. A platinum film 1 x 5 mm., with resistance in the range of 200-700 ohms, is painted on the plane face of a cylindrical glass plug. This plug passes through the tube wall so the film strip fits flush with the inside tube face. When the film is oriented with its long dimension perpendicular to the tube axis, passage of a shock wave produces a detectable resistance change in less than 1 microsecond. The film strip is in series with a battery powered circuit drawing about 10 ma. Resistance changes register as voltage changes.

2. Uses

We employ film strip resistors, because of their simplicity and fast rise-times, to measure average shock speeds, and shock attenuation over known distances, and to activate triggering circuits for the calibrated flash lamp. Time-of-flight measurements can be obtained with one percent

precision from the film strips by using a multichannel time delay. Several film-strip signals may be displayed on a single CRO trace, by means of preset delays of each according to its location. Each film strip signal is sent through a 3 stage amplifier to raise it to the triggering level of the 0-1000 micro-second, three-channel time delay unit. Visual analysis of the CRO trace is simplified by placing a flip-flop lockout circuit after the final stage of each amplifier. The output voltage of the time delay unit is sufficient to trigger the thyatron which initiates the continuum flash-lamp discharge.

C. Pressure Transducers

1. Construction and Description

The pressure transducers are Kistler 601 quartz piezoelectric crystals with sensitivity of 0.5 pico-coulombs per psi. The transducers are mounted in a 1 kg brass plug fitted with Teflon washers and Viton O-rings for vacuum and pressure sealing. Unless the transducer has good mechanical isolation, elastic waves in the shock tube walls will excite the characteristic ringing frequency of the crystal. Transducer outputs are fed with low capacitance cable into Kistler 501 charge amplifiers. These impedance-matching units provide time response of less than 1 micro-second. Amplifier outputs are recorded on a Tektronix 555 dual-beam oscilloscope.

2. Uses

Pressure transducers are employed to measure pressures behind the incident and reflected shocks. The transducers (and associated circuitry) have a time response of one micro-second and the time available for measurement in these shock regions is of order 100-300 micro-seconds. With proper calibration, and good mechanical isolation from the tube walls, pressures can be measured to 4-5%.

D. Wave Speed Photography

1. The Rotating Drum Camera

Rotating drum cameras provide a time-resolved record of events by rapidly sweeping film across the focal plane. The drum camera cylinder is machined from an aluminum billet, has a 4.1" inside diameter and uses 120 size film. A Dumore 1/2 HP motor drives the drum, which is mounted on a Dumore quill. Typical linear film speed is 0.12 mm/micro-sec. A magnetic pickup counts drum revolutions from a magnetic pin inserted in the drive shaft. The present lens is f/6.3 and has 6.6" focal length.

2. Windows and Slits

Two plexiglass windows, 1-1/4" thick and 4" long, are mounted on opposite sides of the test section. Their field of view includes

the tube's reflecting plane and 4" of the tube upstream from it. The windows are O-ring sealed and have inside faces fitting flush with the inside tube walls to 0.005". The orientation of the drum camera optical axis with respect to the tube axis is determined by the reversible light path method. Slits run the length of the window and have micrometer adjustment for closing and opening.

3. Use

Analysis of drum camera photographs gives local incident and reflected shock velocities, and the duration in steady state of the region behind the reflected shock, to better than 1%. Flow velocities behind primary (and reflected) shocks may be determined to 1-4% from drum camera photographs. Figure 9 is a typical wave speed photograph showing the process of shock reflection. Methane (or some other light hydrocarbon) must often be added to the carrier gas, in order to make the shocks self-luminous. Shocks in argon with incident Mach numbers 6.5-9.9 required addition of 20-40 microns Hg of methane.

E. Spectrographs

1. Description

The spectrograph in current use with the shock tube was constructed for temporary service in obtaining time-integrated survey spectra. It has

a speed of $f/22$ and a dispersion of $55 \text{ \AA}/\text{mm}$.

We will soon have in operation a Jarrell-Ash model 75,000 fast spectrograph. It has an effective speed of $f/6.3$, a resolution of roughly 1 \AA in first order, and a linear dispersion of $20 \text{ \AA}/\text{mm}$. Useful range is $2800-7000 \text{ \AA}$.

Aside from time-integrated survey spectra, three types of time resolution will be used to get quantitative intensity measurements.

- (i) A rotating drum camera will be focused on (or placed into) the spectrograph's image plane. A drum camera using 70 mm spectroscopic film is nearing completion.
- (ii) A fast shutter will be operated in front of the spectrograph slit.
- (iii) Multi-channel photoelectric recording is available by means of a device designed by Mr. R. Lincke of the Maryland Physics Department.

2. Use

Absolute line intensity measurements will be correlated with source data to deduce atomic oscillator strengths. Estimates of source temperature can be made from relative line intensities. Time-resolved spectroscopy not only separates the emission from primary and reflected

shock regions but also provides data on relaxation to thermal equilibrium within any one of these regions. Stark broadening profiles, especially of H_{β} , contain information about electron densities in the gas. In conjunction with a calibrated, high temperature continuum flash lamp, the spectrograph is used to measure source temperature by the sensitive line-reversal method.

F. Calibrated High Intensity Flash Lamp

1. Description

A calibrated, high intensity, continuum discharge lamp is being developed by Dr. G. Charatis and others at the Institute for Fluid Dynamics and Applied Mathematics, University of Maryland. A 50.5 micro-farad capacitor bank, operated at 5-10 KV, is discharged across a cylindrical channel at a few millimeters air pressure. The useful duration of luminosity is 20-60 microseconds. Equivalent black body temperatures of 40,000 to 70,000° K are produced over portions of the discharge cycle. The lamp is calibrated against carbon-arc craters and pyrometer tungsten strip lamps.

2. Use

The flash lamp emits a continuum whose brightness is known as a function of time. When reversal occurs, the temperature of the shock tube gas is equal to that of a black body having the observed brightness

at that wavelength. The reversal point can be observed with high precision, so that shock tube temperatures are measured to essentially the precision of the flash lamp calibration.

VI. SHOCK TUBE RESULTS

A. Performance of the Vacuum System

Leak rates were measured with Pirani gauges and checked against an ionization gauge. Separation of leak sources into real leaks and virtual leaks, (out-gassing), was made by observing tube pressure as a function of time over periods of tens of hours. Mean leak rate for the shock tube is 0.02 microns/min., even though a few small leaks can still be seen with a helium mass spectrograph detector. At this leak rate, the expansion section and manifold base pressure is maintained at 2×10^{-6} mm/Hg, as measured in the vacuum gauge submanifold.

After 24 hours exposure to air, 9 hours are required to reach base pressure. After 24 hours exposure to one atmosphere of dry nitrogen, 2 hours are needed to reach base pressure. The pump-down times encountered in routine cyclic operation of the system are as follows: 45 minutes required to reach base pressure after 5 minutes exposure to atmosphere after a shot; 15 minutes required to reach base pressure after 5 minutes

exposure to one atmosphere of super-dry nitrogen. These data show that routine back-filling with dry nitrogen will allow us to make about ten shots a day.

B. Diaphragm Testing

Copper, annealed mild steel, and several aluminum alloys were tested as diaphragm materials. Dead soft aluminum (Alcoa #AL-1100) consistently gave best reproducibility of bursting pressure and superior petaling configurations. Diaphragms are cut from masked aluminum sheet and turned to a 6-1/2" diameter, 20 to 40 at a time, on a lathe. Grooves are cut with a V-shaped milling wheel so that they join the diagonally opposite inside corners of the tube cross section. If groove depths are held to 0.001" tolerance, and the orientation is symmetric about the roll-marks of the diaphragm material, the r.m.s. scatter in bursting pressure at 600 psi is ± 5 psi.

Bursting pressure is strongly dependent both on diaphragm thickness and the ratio of groove-depth to diaphragm thickness. Diaphragm petaling behavior also depends on these two parameters. The data are collected in Figure 8.

C. Hydrodynamic and Spectroscopic Performance of Shock Tube

1. Purpose of Preliminary Hydrostatic Testing

Preliminary hydrodynamic tests demonstrated the tube's suitability as a spectroscopic source. The criteria used were:

- (a) Is a clean (spatially well defined) incident shock wave formed?
- (b) Is there an observable lifetime, in steady state, of the high temperature gas behind the reflected shock?
- (c) Does the gas behind the reflected shock exhibit large-scale mixing or is it macroscopically homogeneous?
- (d) How well does observed shock behavior agree with the one-dimensional theory predictions?

2. Data From Rotating Drum Camera Photographs

Hydrogen driven shocks in argon were studied with the rotating drum camera. Incident shock Mach numbers ranged from 6.5-9.9. Initial pressures of 1-60 mm. Hg and 120-1800 psi were covered for argon and hydrogen, respectively.

Wave speed photographs showed incident and reflected shock fronts to be well-defined spatially. The resolution of our optics is 0.5 mm. A typical wave speed photograph, showing incident and reflected

shock, is given in Figure 9.

The gas behind the reflected shock, observed at the point 5 mm. upstream from the tube's reflecting plane, emitted a steady level of visible light for periods of 60-280 microseconds.

These times are considered adequate for establishment of local thermal equilibrium. Duration of the luminosity t_0 depends upon initial argon pressure P_4 and incident shock Mach number M_1 . The data summarized in Figure 11 gives M_1 , but not P_4 , dependence of t_0 .

Macroscopic mixing behind the reflected shock was observed in some cases when initial argon pressure exceeded 40 mm. Hg. No mixing was found for initial pressures of argon below 40 mm. Hg.

Recorded primary shock Mach numbers, u/c_0 , are given as functions of the initial pressure ratio, P_4/P_1 , in Figure 10. On the same axes are also plotted the primary Mach numbers predicted by the one dimensional, ideal flow theory for real argon gas.

Reflected shock speeds were measured with accuracies of 3-6%. Without additional data on the primary flow field, (i.e., to permit a determination of reflected shock Mach number), we simply choose the observed absolute reflected shock speed, V , to check against theoretical predictions. Both the observed and predicted values of V are plotted

as functions of primary shock Mach number in Figure 11. Increasing departure from ideal behavior is obtained with higher Mach numbers, due to both the increase in wall effects at low P_1 and the increase in ionization behind the reflected shock.

Small concentrations of methane were added to the argon to increase the luminosity from various shock regions. Methane partial pressures were kept at 20-40 microns Hg to avoid complicating the analysis of the tube hydrodynamics. In spite of the admixed methane, luminosity levels were often low, particularly for shocks below $M=7.5$, and most drum camera photographs lack sufficient density and/or contrast for accurate reading of both incident and reflected shocks.

3. Pressure Transducer Performance

a. Calibration

Transducers are calibrated in a small, pressurizable chamber sealed by a cellophane diaphragm. Breaking the diaphragm presents the transducer with an abrupt pressure change, simulating passage of a wave in the shock tube. Charge amplifier outputs are plotted against known pressure change. Linear dependence, with a slope of 0.08 ± 0.001 volt/psi, is observed over the range of pressure changes of interest.

4. Pressure Data from The Shock Tube

Transducers mounted in the shock tube have not delivered usable pressure data. The signals of interest are swamped by the crystal's characteristic ringing. This ringing, at 140-160 kc., persists without

appreciable damping for periods exceeding those available for pressure measurements in the flow regions of interest. Common experience with transducers indicates that we must avoid exciting the crystal ringing frequency by providing better mechanical isolation from the tube walls.

5. Spectroscopic Data

The spectroscopic data consists so far only of time-integrated exposures. The limited capabilities of the current spectrograph, rather than a lack of high intensity radiation, have prohibited quantitative time-resolved spectroscopy.

Shocks with incident Mach numbers in the range of 6.5-10, propagated in 5-25 mm. Hg of commercial argon plus 20 - 40 x 10⁻³ mm. Hg of methane, produced strong spectral lines on the time-integrated films. In the region 4300-6800 Å, the following elements were observed: aluminum, argon, hydrogen, krypton, sodium and xenon.

The emission of hydrogen, krypton and xenon lines is noteworthy because partial pressures of these gases are of order 10⁻³ of the argon carrier gas pressure.

VII. RESEARCH FOR THE CURRENT YEAR

Work now under way is directed towards:

- (1) The perfection of adequate shock tube instrumentation.
- (2) Decreasing the vacuum pump-down time and static leak rate of the system.
- (3) Making provisions for the accurate and convenient metering and storage of test and carrier gases.
- (4) Accurately recording the shock tube's hydrodynamic behavior and studying the time-behavior of the gas behind the reflected shocks.

A. Development Work in Progress

1. Electronics for securing 1% accuracy shock speed measurements, independent of shock luminosity, are nearing completion.
2. Several alternate schemes for mechanically isolating the pressure transducers are being tried. The enduring problem is to obtain good mechanical isolation from the tube walls without sacrificing vacuum and pressure integrity.
3. All known leak sources are being eliminated. Most of these are associated with commercially obtained vacuum valves. The most formidable job is the construction of a 3-1/2" piston-valve to replace the large Arrowflow valve connecting the vacuum system with the shock tube.

4. Facilities for the metering, mixing and storage of carrier and test gases are being improved by the use of fine metering valves, positive shut-off valves, stainless steel plumbing and chromium-plated storage tanks.

5. Under construction are a carriage mounting and a vibration-isolated rotating drum camera for use with the f/6.3 Jarrell-Ash #75,000 spectrograph.

B. Experiments in Progress

1. Incident and reflected shock Mach numbers are being measured to 1-2% by an improved rotating drum camera. Hydrogen driven shocks in neon and argon are being studied over a wide range of initial pressures.

2. Incident and reflected shock flow velocities are also being studied with the improved rotating drum camera. Finely ground cesium nitrate, adhering to a thin thread, is introduced at an appropriate point in the shock's path. Upon passage of the shock front, some of the cesium nitrate is vaporized in the hot flow and quickly assumes the local flow velocity. Since cesium is highly luminous, its progress is recorded by the rotating drum camera.

3. By suitably combining diaphragm thickness and groove depths, a large number of diaphragms can be prepared all having the same breaking pressure but varying in breaking kinematics. We are looking for the ratio

of groove depth-to-diaphragm thickness that gives the maximum time of observation in the reflected shock region for a given bursting pressure.

4. A selection is being made of the most favorable phototubes (and associated circuitry) for obtaining high time resolution and easy data reduction.

C. Spectroscopic Studies for the Current Year

Within the current year, we plan to advance well into the work described below.

The first two spectroscopic studies are designed to assess our equipment and techniques. First, absolute oscillator strengths will be measured for the Balmer series of Hydrogen, both by emission and by absorption using the continuum lamp. These gf measurements will be compared with the tabulated values, known to better than 1% from perturbation theory. Balmer profiles will also be examined to give emitting gas temperatures and electron densities.

After these preliminaries we will take up the study of absolute oscillator strengths of astrophysical interest. We envision the program roughly as the following:

- (1) Ne I and A I will be remeasured to clarify the results of past work. The best gf -value to work to date still

leaves factor-of-two uncertainties for most visible lines.

- (2) Prominent lines of C I and O I will be re-done for essentially the same reasons.
- (3) Lines of S I will be studied in detail. Sulphur is hard to excite in many sources, but was readily brought out in survey work at Michigan. The results will be compared with Mr. Bridges' work at NBS which uses a stabilized arc. Hopefully we can reduce the present factor-of-six uncertainty in solar abundance by these means.

D. Long-Range Plans for Spectroscopic Measurements

With the completion of the above investigations we intend to pursue the following program

- (1) The halogens will be done using appropriate organic additives. From the Michigan work we know that Cl I and Cl II can be observed under our conditions.
- (2) We will prepare safe procedures for measurements on silicon and phosphorus in 1-2 years' time. This involves overcoming difficulties of hydrolysis and toxicity, but we are confident of the result from our work with chromium carbonyl and R. S. Berry's work with diborane.

(3) Other problems will be studied from time to time:

(a) line broadening parameters will be catalogued whenever line widths are observed to be larger than instrumental profiles,

(b) line strengths will be measured both in emission and absorption whenever optical depths are sufficient for satisfactory precision,

(c) importance of non-coherent terms in the radiative transfer equations will be assessed by means of high intensity illumination over band widths narrow compared to broadest lines,

(d) in certain ranges of flow variables, we will observe transient or steady-state departures for LTE and try to rationalize them with cross section data.

LIST OF FIGURES

- Figure 1 Diagonal View of Shock Tube Facing From Test Section Towards Driver Section
- Figure 2a Schematic Cross Section of Reinforced Driver Section
- Figure 2b Schematic Cross Section of Reinforced Expansion Section
- Figure 3 Close-up of Instrumentation Port, Showing Blank Plug and Retaining Ring
- Figure 4 Exposed Breech Face, Showing Quick-Release Securing Bolts
- Figure 5 The Vacuum System and Main Manifold
- Figure 6 Schematic View of Shock Tube and Associated Equipment
- Figure 7 The Test Section, Showing Spectroscopic Window
- Figure 8 Diaphragm Bursting Pressure As A Function of Groove-Depth to Diaphragm Thickness For Three Thicknesses of Dead-Soft Aluminum
- Figure 9 Enlargement of Wave-Speed Photograph Showing Incident and Reflected Shocks
- Figure 10 Observed and Ideal Incident Shock Mach Numbers Compared as Functions of P_4/P_1
- Figure 11 Observed and Ideal Reflected Shock Speeds V As Functions of Primary Shock Mach Number M_1

Bibliographical Notes

Several reviews of shock tube research, particularly spectroscopic work at high temperatures, have appeared in the past six years (1 - 4). Our work is principally an extension of the program at Michigan (2, 5 - 18). Recent reports (19 - 21) typify developments at other universities. For discussion of specific techniques, various sources will be helpful to the interested reader: electron density measurements by optical interferometry (22,23), temperature measurement by spectral line-reversal (16 - 20, 24 - 26), absolute heterochromatic photometry (14 - 16, 27, 28) and various spectroscopic determinations of the state of hot gases and plasmas (3, 29).

References

1. I. I. Glass and J. G. Hall, Shock Tubes, University of Toronto Institute of Aerophysics Review No. 12 (May 1958) and Section 18, Volume 6, Handbook of Supersonic Aerodynamics, Navord Report 1488 (December 1959).
2. O. Laporte and T. D. Wilkerson, J. Opt. Soc. Am. 50, 1293 (1960).
3. H. R. Griem and A. C. Kolb, Chapter "High Temperature Shock Waves" in Atomic and Molecular Processes (D. R. Bates, ed.) Academic Press (1962).
4. A. G. Gaydon and I. R. Hurle, The Shock Tube in High Temperature Chemical Physics, Chapman and Hall Ltd., London (1963).
5. R. N. Hollyer, Jr., A. C. Hunting, Otto Laporte, E. H. Schwarz and E. B. Turner, Phys. Rev. 87, 911 (1952).
6. R. N. Hollyer, A. C. Hunting, O. Laporte and E. B. Turner, Nature 171, 395 (1953).
7. Eugene B. Turner, "The Production of Very High Temperatures in the Shock Tube with an Application to the Study of Spectral Line Broadening", Ph.D. thesis and University of Michigan Engineering Research Institute Report No. 2189-2-T, AFOSR TN-56-150, ASTIA-AD 86309 (May 1956).
8. E. B. Turner, Phys. Rev. 99, 633 (1955).
9. G. Charatis, L. R. Doherty and T. D. Wilkerson, J. Chem. Phys. 27, 1415 (1957).
10. G. Charatis and T. D. Wilkerson, Bull. Am. Phys. Soc. 3, 292 (1958).

11. G. Charatis and T. D. Wilkerson, *Phys. Fluids* 2, 578 (1959).
12. L. R. Doherty, *Bull. Am. Phys. Soc.* 5, 131 (1960).
13. T. D. Wilkerson, *Bull. Am. Phys. Soc.* 5, 131 (1960).
14. L. R. Doherty, "Measurement of Atomic Transition Probabilities by means of a Shock Tube", Ph.D. thesis, University of Michigan (June 1961).
15. T. D. Wilkerson, "The Use of the Shock Tube as a Spectroscopic Source with an Application to the Measurement of *gf*-Values for Lines of Neutral and Singly Ionized Chromium", Ph.D. thesis and University of Michigan, Office of Research Administration Report No. 02822-3-T, AFOSR 1151, (June 1961).
16. G. Charatis, "Shock Tube Determination of Chromium *gf*-Values", Ph.D. thesis, University of Michigan (December, 1961).
17. G. Charatis and T. D. Wilkerson, *Phys. Fluids* 5, 1661 (1962).
18. G. Charatis and T. D. Wilkerson, Proceedings of the Sixth International Conference on Ionization Phenomena in Gases, Vol. III, p. 401, S.E.R.M.A., Paris, France (July, 1963).
19. P. L. Byard, R. E. Roll and A. Slettebak, "The Design and Construction of a Luminous Shock Tube for Spectroscopic Investigations of High-Temperature Gases; Preliminary Results for Some Elements of Astrophysical Interest", Ohio State University Research Foundation Report No. AFCRL-63-252 (January, 1963).
20. E. M. Reeves and W. H. Parkinson, "Temperature Measurements for Shock Heated Powered Solids", Harvard College Observatory Scientific Report No. 1 (January, 1964).

21. H. Kawada, "A 7 cm x 7 cm Shock Tube at the Department of Aeronautics, University of Tokyo", Research Memorandum No. 5, T. Moriya Memorial Seminar for Aerodynamics, University of Tokyo (January, 1964).
22. R. A. Alpher and D. R. White, *Phys. Fluids* 2, 162 (1959).
23. D. T. Llewellyn-Jones, S. C. Brown and G. Bekefi, Proceedings of the Sixth International Conference on Ionization Phenomena in Gases, Vol. IV, p. 157, S.E.R.M.A., Paris, France (July, 1963).
24. H. Kohn, *Phys. Z.* 33, 957 (1932).
25. F. S. Faizullov, N. N. Sobolev and E. M. Kudryatsev, *Opt. i. Spektr.* 8, 311, 400 (1960).
26. J. G. Clauston, A. G. Gaydon and I. R. Hurle, *Proc. Roy. Soc.* A252, 143 (1959).
27. G. R. Harrison, *J. Opt. Soc. Am.* 19, 267 (1929); 24, 59 (1934).
28. J. Euler, *Ann. Physik* (6) 11, 203 (1953); (6) 14, 10 (1954).
29. H. R. Griem, Plasma Spectroscopy, to be published by McGraw-Hill (1964).

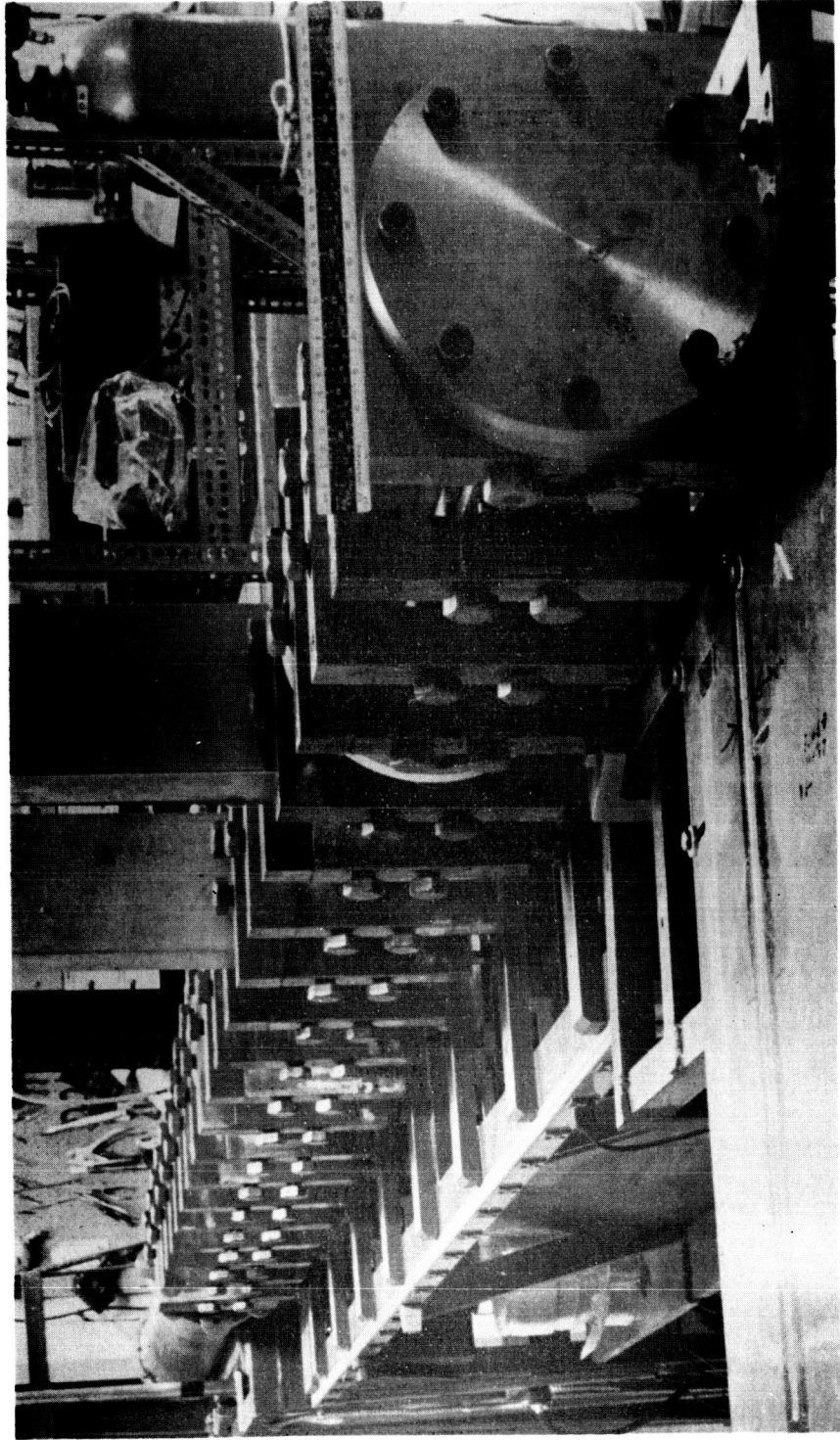
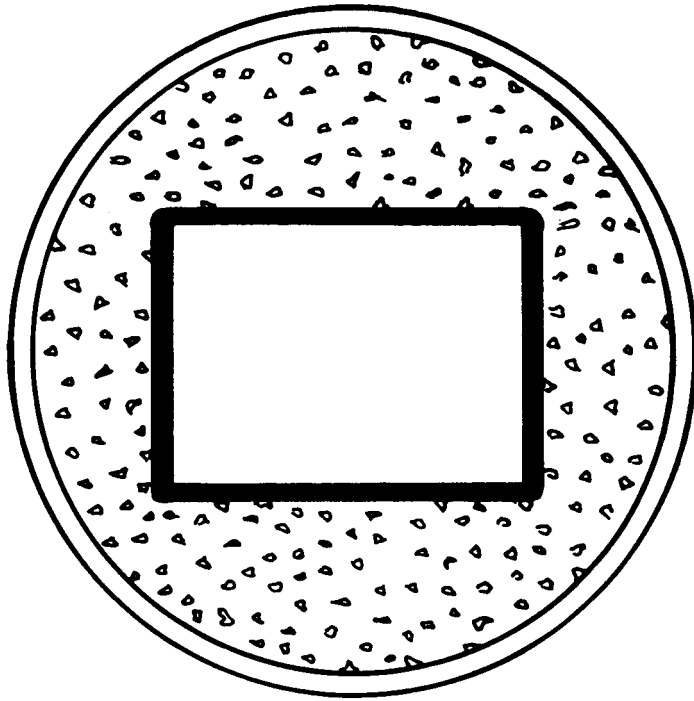
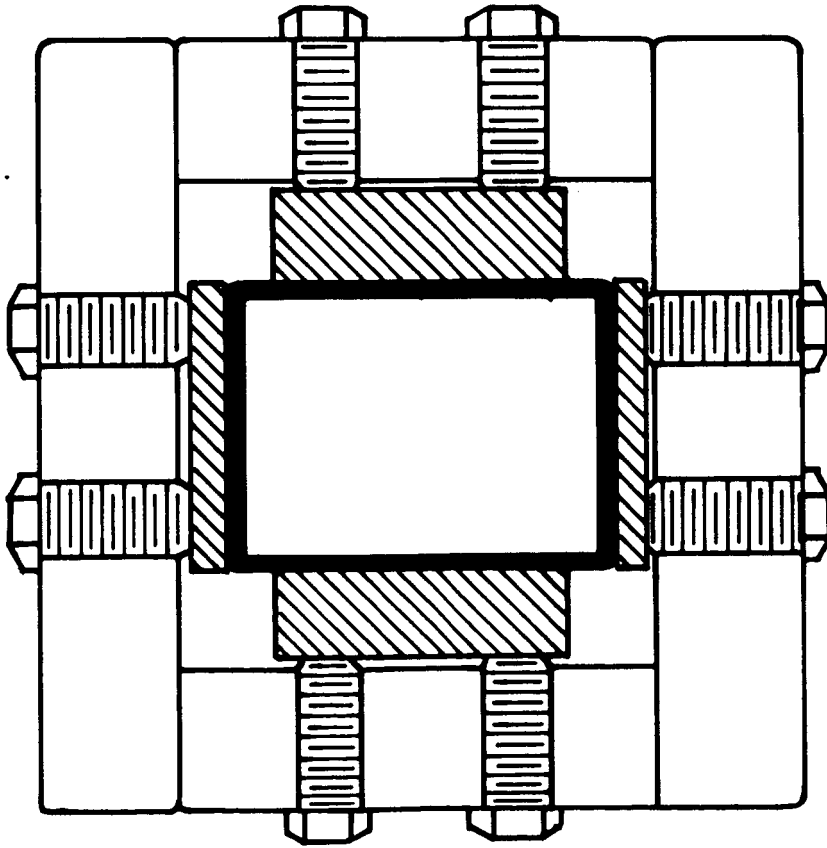


Figure 1



MATERIALS:

■ RESISTANCE WELDED MILD STEEL TUBE
 THICKNESS .180"

▨ HIGH DENSITY CONCRETE

▧ MILD COLD ROLLED STEEL BAR STOCK

SCALE: HALF SIZE

Figure 2a

Figure 2b

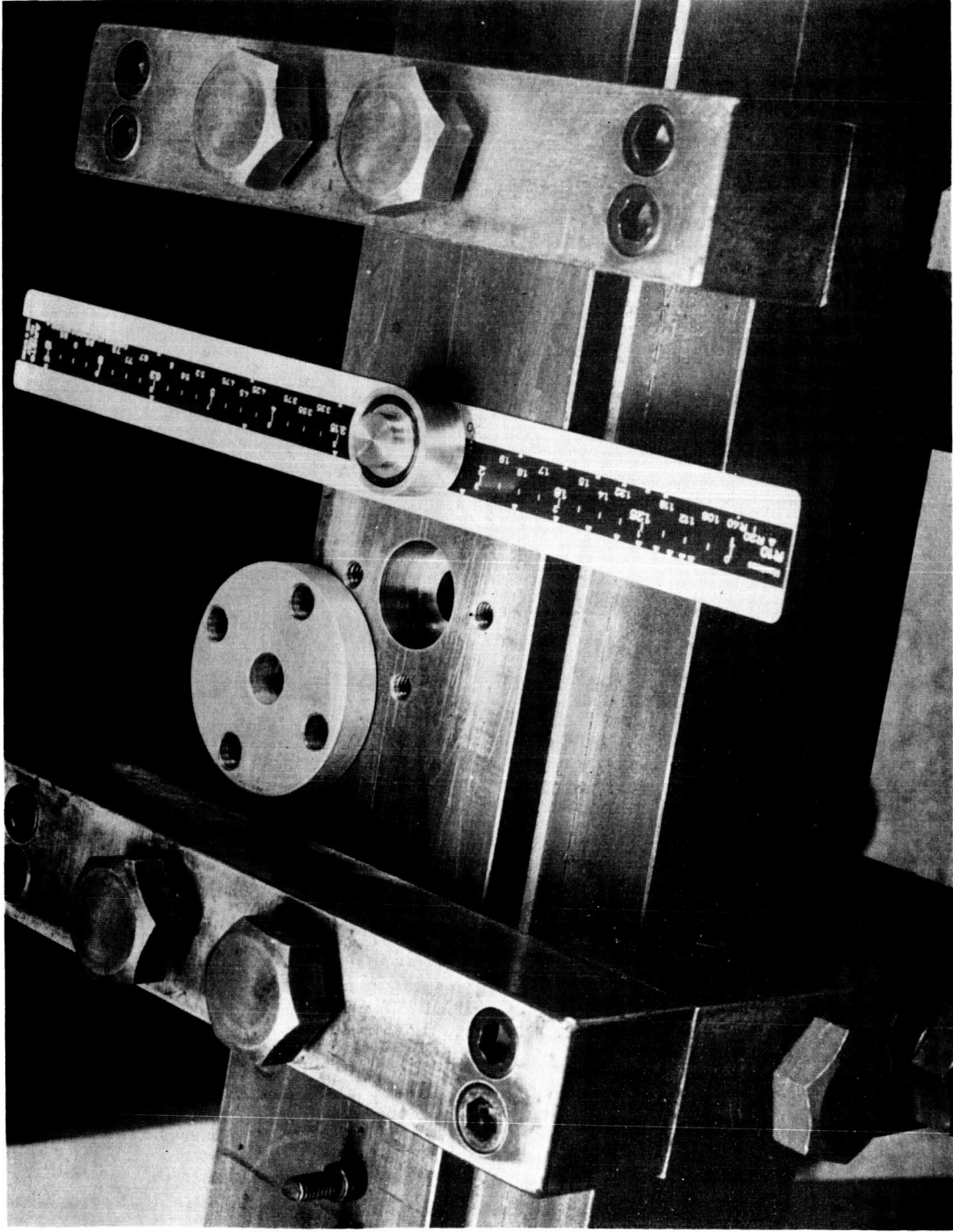


Figure 3

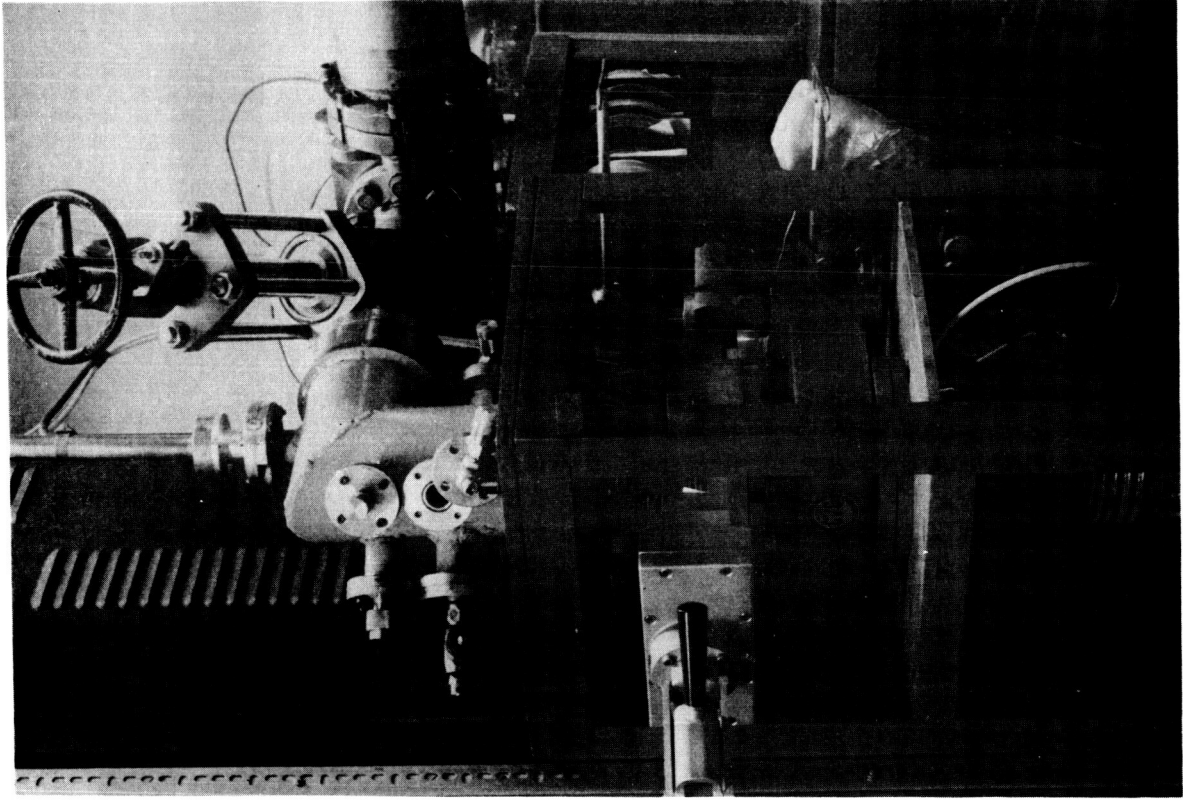


Figure 5

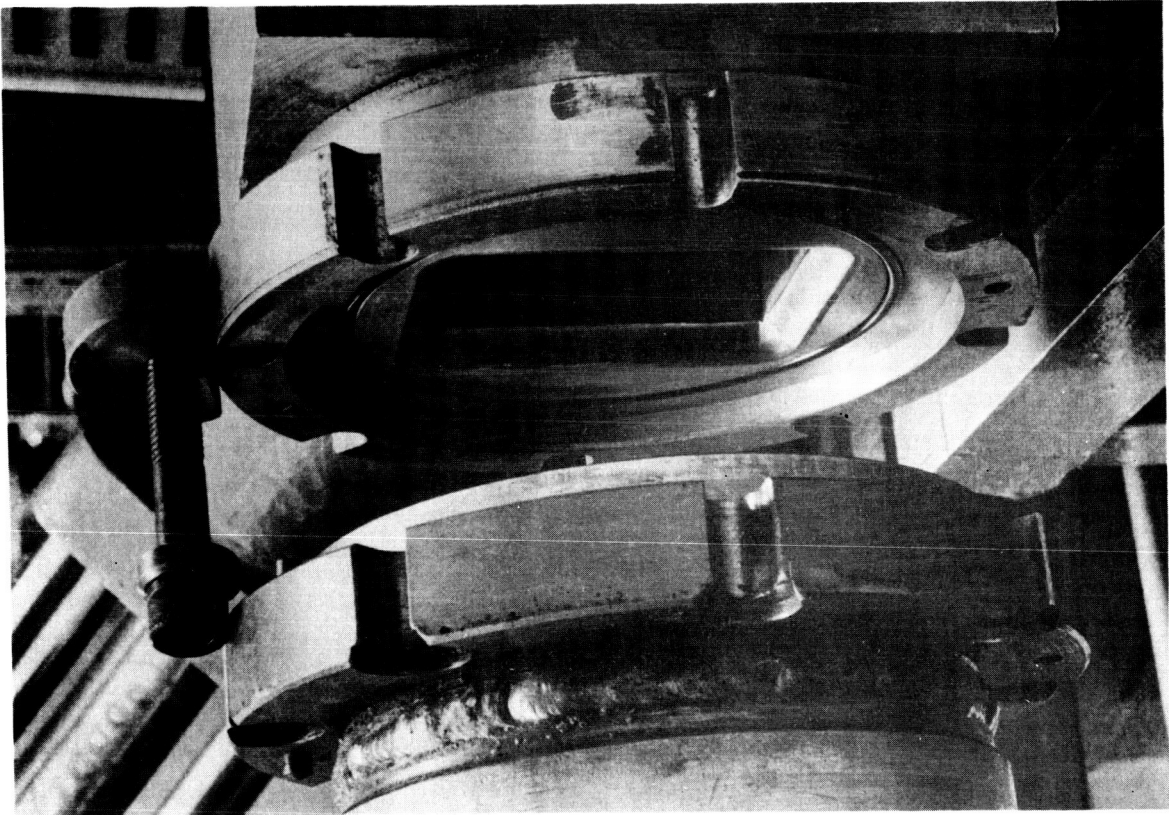
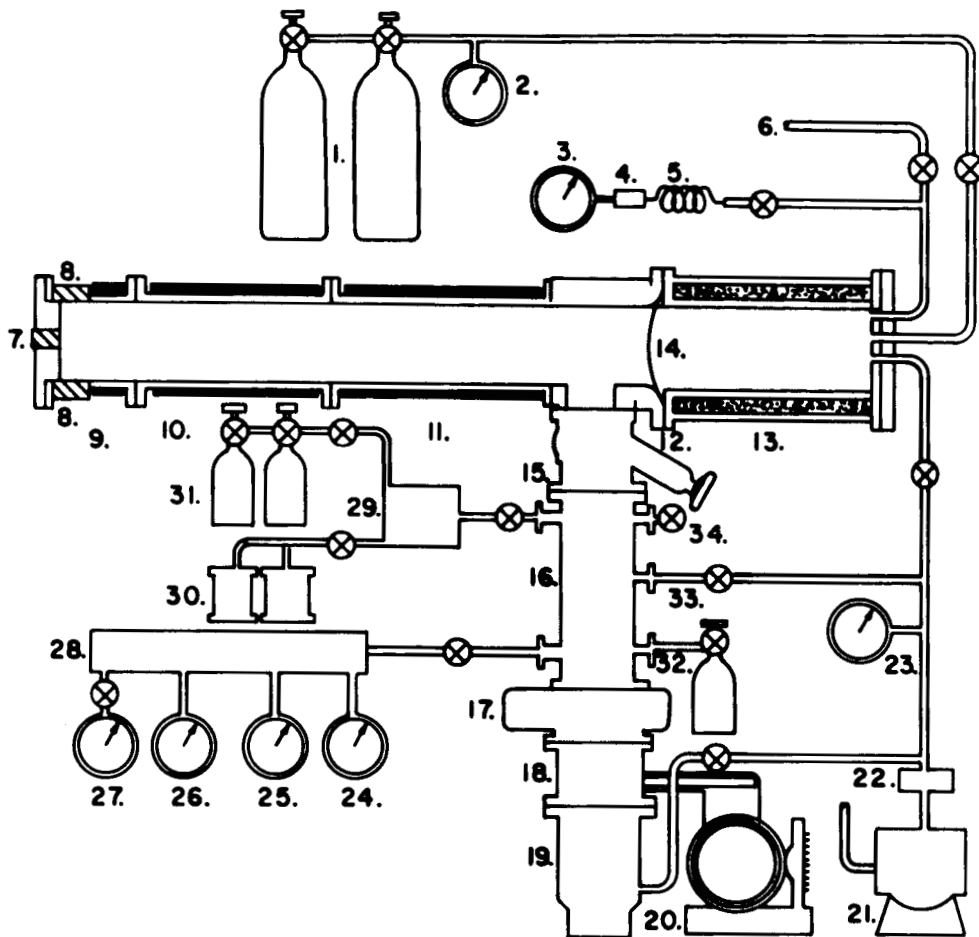


Figure 4



- | | |
|--|--|
| 1. 2000psi DRIVER GAS CYLINDERS | 18. VEECO 4" BAFFLE |
| 2. TANK PRESSURE GAUGE | 19. 4" PMC-721 DIFFUSION PUMP |
| 3. HEISE 0-2000psi DRIVER PRESSURE GAUGE | 20. 1/4 hp FREON COMPRESSOR |
| 4. SURGE-TANK GAUGE SHOCK PROTECTION | 21. DUO-SEAL 20 CFM PUMP |
| 5. 6' STAINLESS STEEL CAPILLARY TUBE | 22. KANE MOLECULAR SIEVE |
| 6. H ₂ VENT TO OUTDOORS | 23. PIRANI FORE-LINE GAUGE |
| 7. WINDOW FOR AXIAL VIEWING | 24. 0-20mm DIAPHRAGM GAUGE |
| 8. WINDOW FOR LATERAL VIEWING | 25. CVC IONIZATION GAUGE |
| 9. TEST SECTION | 26. AUTO-VAC PIRANI GAUGE |
| 10. FIRST EXPANSION CHAMBER | 27. N ₂ -TRAPPED McLEOD GAUGE |
| 11. SECOND EXPANSION CHAMBER | 28. GAUGE SUB-MANIFOLD |
| 12. BREECH SECTION | 29. MIXING SUB-MANIFOLD |
| 13. DRIVER SECTION | 30. STORAGE CYLINDERS |
| 14. DIAPHRAGM | 31. CARRIER AND TEST GAS CYLINDERS |
| 15. "ARROW-FIO" Y-VALVE | 32. N ₂ -BACK FILLING STATION |
| 16. MAIN MANIFOLD | 33. ROUGHING PUMP LINE |
| 17. VEECO GATE VALVE | 34. He LEAK-TESTING ACCESS PORT |

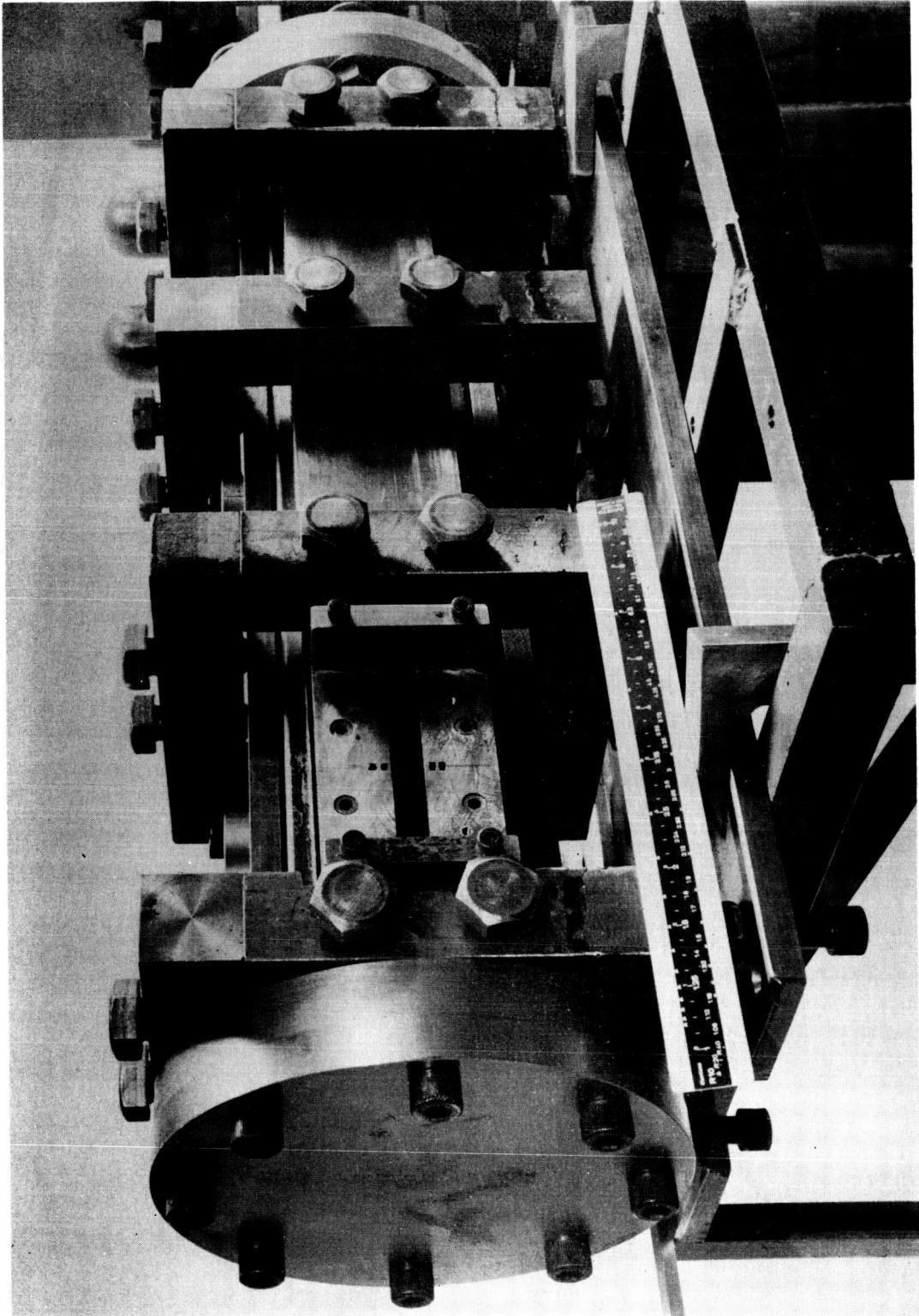
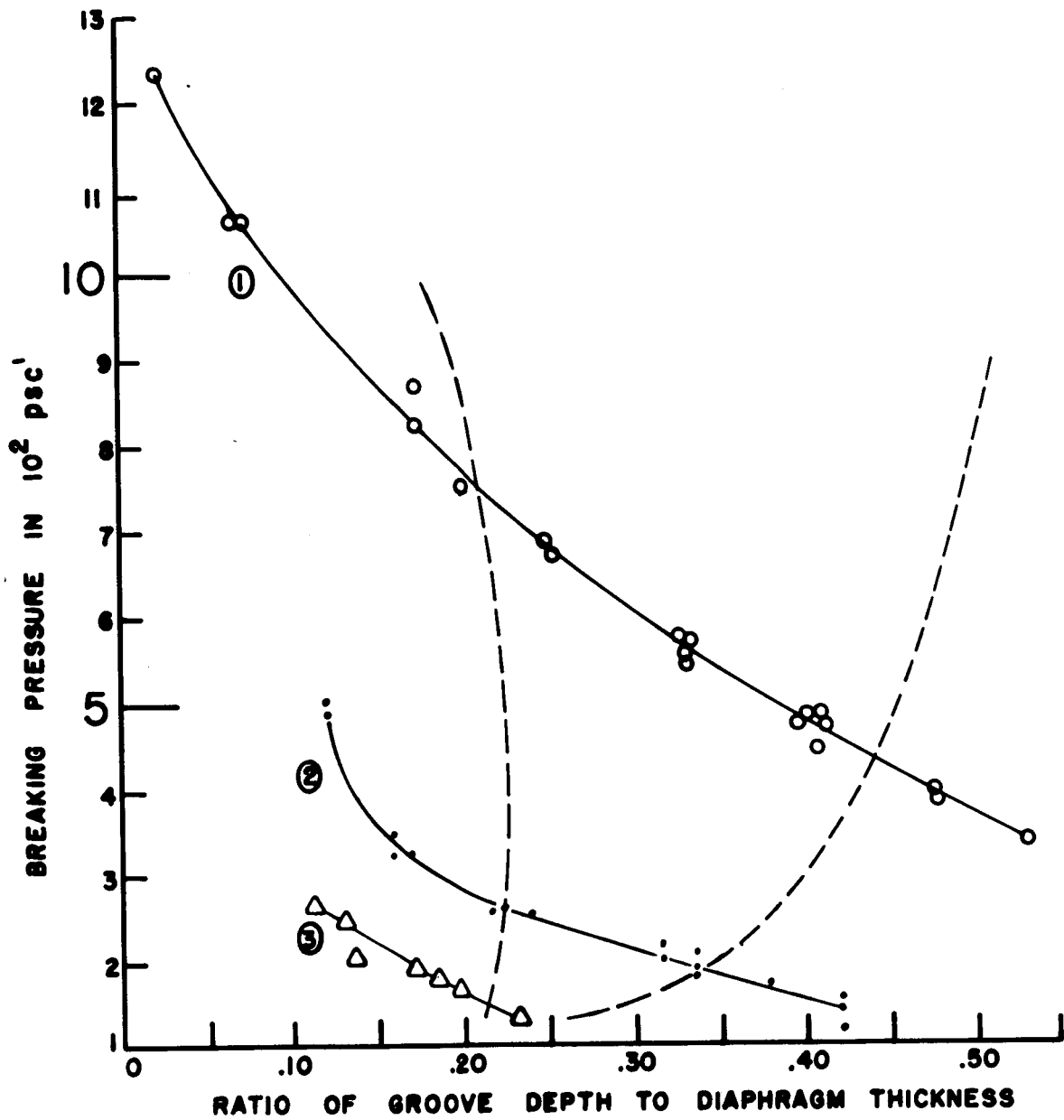


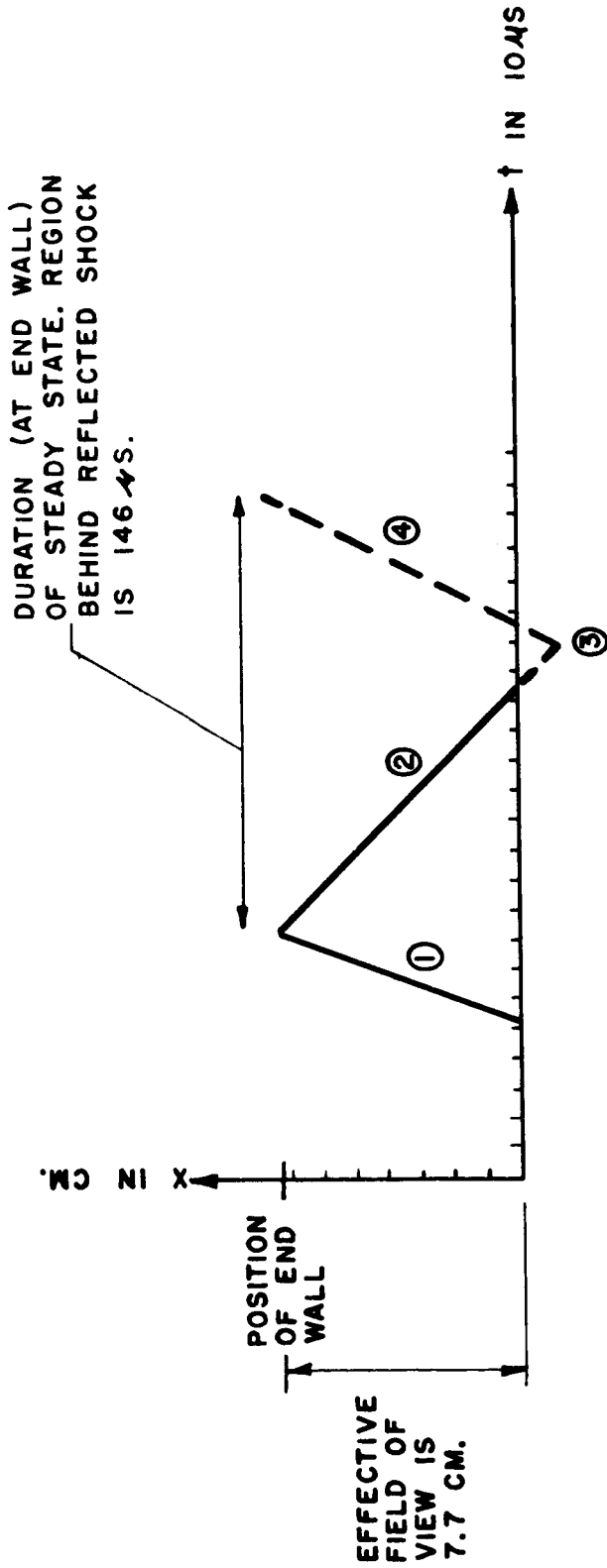
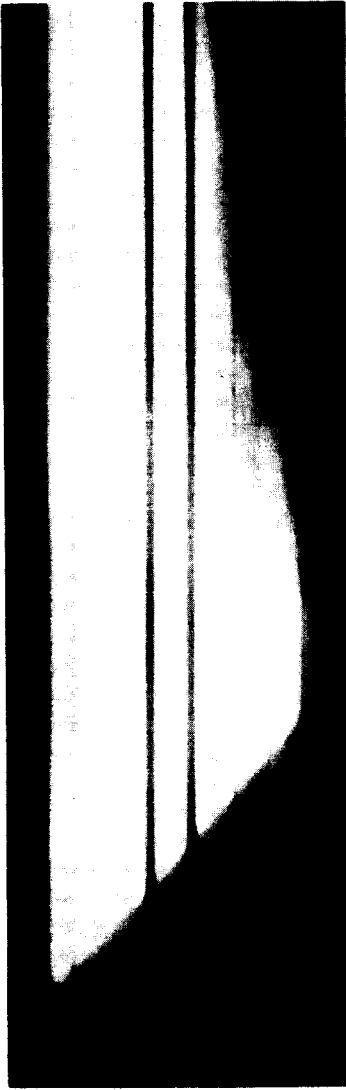
Figure 7



IN REGION BETWEEN DASHED LINES DIAPHRAGMS WILL OPEN TO $\geq 90\%$ OF TUBE-EXPOSED AREAS.

DIAPHRAGM THICKNESS: ① = .125"
 ② = .080"
 ③ = .060"

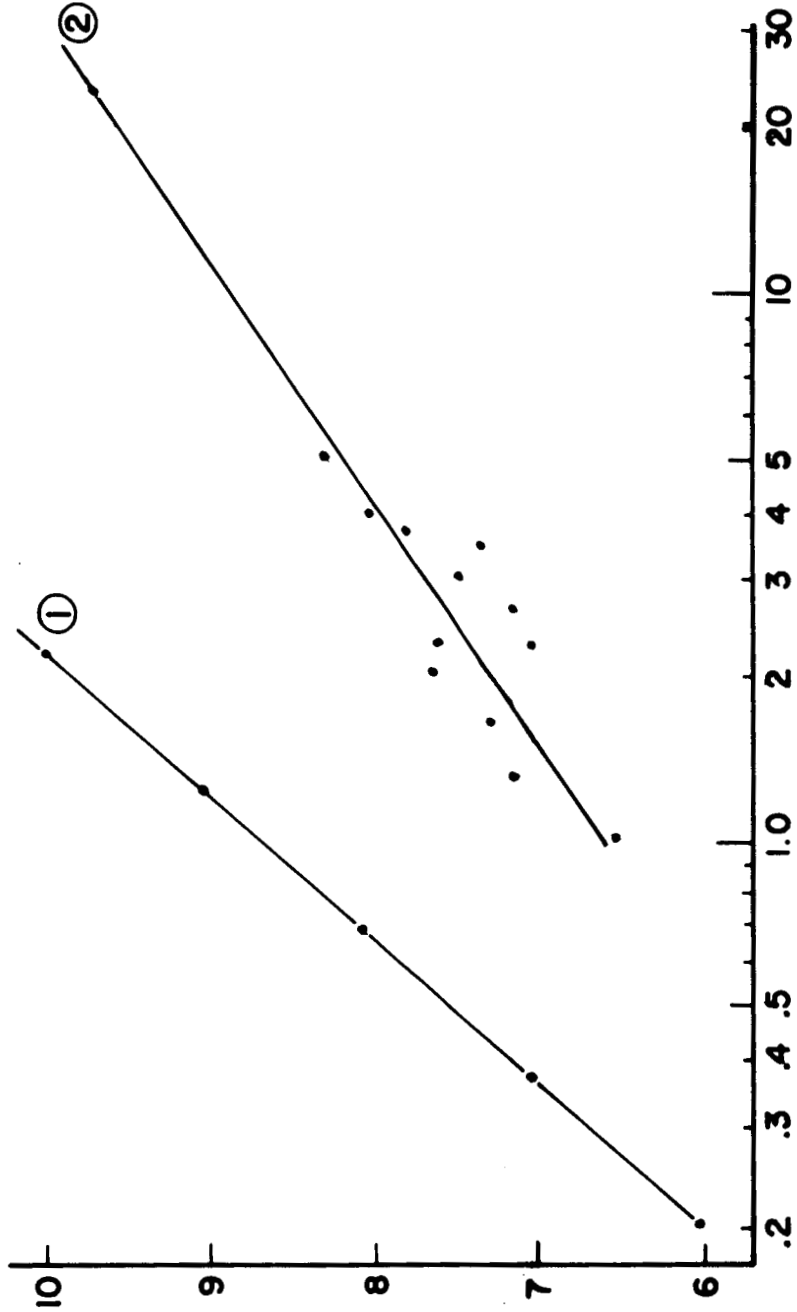
Figure 8



- ① PRIMARY SHOCK.
- ② REFLECTED SHOCK.
- ③ REFLECTED SHOCK INTERACTS WITH CONTACT SURFACE (NOT IN FIELD OF VIEW).
- ④ WAVE RESULTING FROM 3 DISRUPTS REGION BEHIND REFLECTED SHOCK.

Figure 9

INCIDENT SHOCK MACH NUMBER AT POSITION
OF SPECTROSCOPIC WINDOWS.

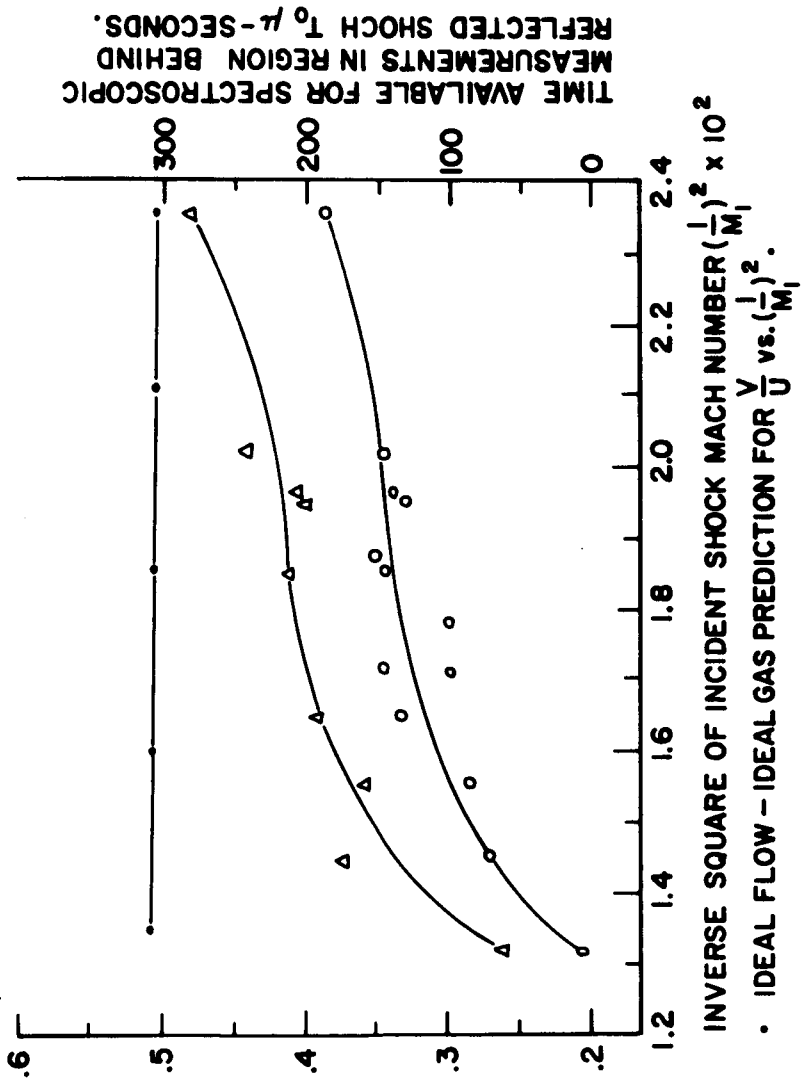


$P_4/P_1 \times 10^3 =$ INITIAL PRESSURE RATIO

- ① PREDICTED BY RANKINE-HUGONIOT EQUATIONS FOR IDEAL H₂ DRIVEN SHOCKS PROPAGATED IN NON-IONIZABLE ARGON.
- ② LEAST SQUARES FIT FOR OBSERVED SHOCKS USING COMMERCIAL GRADE HYDROGEN AND ARGON.

Figure 10

RATIO OF REFLECTED TO INCIDENT SHOCK SPEEDS $\frac{U}{V}$



TIME AVAILABLE FOR SPECTROSCOPIC MEASUREMENTS IN REGION BEHIND REFLECTED SHOCK T_0 μ -SECONDS.

INVERSE SQUARE OF INCIDENT SHOCK MACH NUMBER $(\frac{1}{M_1})^2 \times 10^2$

- IDEAL FLOW - IDEAL GAS PREDICTION FOR $\frac{V}{U}$ vs. $(\frac{1}{M_1})^2$.
- OBSERVED $\frac{V}{U}$ vs. $(\frac{1}{M_1})^2$ FOR COMMERCIAL GRADE ARGON
- △ OBSERVED τ_0 vs. $(\frac{1}{M_1})^2$ FOR COMMERCIAL GRADE ARGON AT POSITION OF REFLECTING WALL.

Figure 11